NACA

RESEARCH MEMORANDUM

HEAT TRANSFER TO SURFACES AND PROTUBERANCES IN A

SUPERSONIC TURBULENT BOUNDARY LAYER

By Paige B. Burbank and H. Kurt Strass

Langley Aeronautical Laboratory
Langley Field, Va.

NATIONAL ADVISORY COMMITTEE
FOR AERONAUTICS
WASHINGTON
July 14, 1958

NATIONAL ADVISORY COMMITTEE FOR AERONAUTICS

RESEARCH MEMORANDUM

HEAT TRANSFER TO SURFACES AND PROTUBERANCES IN A

SUPERSONIC TURBULENT BOUNDARY LAYER*

By Paige B. Burbank and H. Kurt Strass

SUMMARY

The presence of large protuberances that are only partially
immersed in a turbulent boundary layer effects a large increase in heat
transfer upstream and on each side of the protuberance wake. Extreme
care must be taken in locating a protuberance in the influence of
another one. The ratio at a particular thermocouple of the heat-
transfer coefficient for the flat plate with the protuberance to the
heat-transfer coefficient of the flat plate alone can be as great as
12 in the more adverse location.

INTRODUCTION

The importance of minimum weight and maximum fuel volume has led
in some cases to the location of major piping on the outer shell of
large missiles. In the absence of a suitable theory for calculating
the heat transfer to protuberances totally or partially immersed in a
turbulent boundary layer, tests were conducted to determine experi-
mentally the distribution of heat transfer to the protuberance and the
adjacent skin area. Tests were conducted on several configurations
with circular cylinders mounted normal to a flat plate to simulate
antennas or externally mounted pipes.

SYMBOLS

N_{St} Stanton number

d   diameter, 2.8 in.

h   heat-transfer coefficient

*Title, Unclassified.

h_L heat-transfer coefficient based on free-stream conditions for laminar flow on cylinder of infinite length

h_o heat-transfer coefficient of flat plate alone

M   Mach number

R   Reynolds number

T   wall temperature

δ boundary-layer thickness

ψ meridian angle

Subscript:

x   distance from leading edge of flat plate

MODEL DESIGN

The perspective drawing in figure 1 illustrates the instrumented cylinder mounted on the 4- by 10-foot flat plate that spans the test section along the horizontal center plane of the Langley Unitary Plan wind tunnel. A 1-inch-wide band of No. 60 carborundum grains located 4 inches rearward of the leading edge was used to insure a turbulent boundary layer. The leading-edge wedge was alined so that no flow deviation occurred on the test surface, and pneumatic seals prevented flow around the edges of the plate.

The instrumented portion of the flat-plate surface is composed of two interchangeable panels, each instrumented with iron-constantan thermocouples, having a uniform skin thickness of 0.050-inch stainless steel, and insulated from the support structure by a 1/2-inch honeycomb of Fiberglas. The panel used for a protuberance support has 84 thermocouples; the filler panel, 9 thermocouples.

The instrumented cylinder also constructed of stainless steel has a height of $12\frac{1}{2}$ inches, a diameter of 2.8 inches, and a uniform skin thickness of 0.050 inch. The cylinder is insulated from the flat plate by a 0.11-inch sheet of Micarta. Twenty-four thermocouples were located along the stagnation line and 45° and 90° from the stagnation line, as shown in figure 1.

METHOD OF DATA REDUCTION

The heat-transfer coefficients are obtained from the basic heat-transfer equation by using the transient temperatures resulting from a stepwise increase in the stagnation temperature. The individual ratios of equilibrium temperature to stagnation temperature are determined prior to the stagnation temperature bump. The transient thermocouple measurements are obtained every 1/2 second for 1 minute on a Consolidated Engineering Corporation Millisadic.

RESULTS AND DISCUSSION

The heat-transfer coefficients were first determined for the flat plate alone at Reynolds numbers per foot varying from 1.33×10^6 to 3.98×10^6 and at free-stream Mach numbers of 2.65 and 3.51. The resultant Stanton numbers for locations within 5 inches of the center line of the flat plate are shown for $M = 2.65$ at $R = 2.58 \times 10^6$ per foot and $M = 3.51$ at $R = 2.86 \times 10^6$ per foot in figure 2. The experimental Stanton numbers for the plate are somewhat lower (8 to 25 percent) than predicted by the Van Driest theory. Similar differences have frequently been noted by others.

The results of the protuberance tests are presented as a ratio at a particular thermocouple of the heat-transfer coefficient for the flat plate with the protuberance to the heat-transfer coefficient of the flat plate alone. This ratio will be referred to hereinafter as h/h_o.

The heat-transfer distribution is shown in figure 3 for a single cylinder mounted on the flat plate for a free-stream Mach number of 3.51 and a Reynolds number of 23.4×10^6.

The boundary-layer thickness, calculated by the method outlined in reference 1, at the position of the cylinder is 43 percent of the cylinder diameter. The distribution of thermocouple locations, denoted by crosses, permits considerable freedom in determining the location of the h/h_o contours; the regions, therefore, are representative rather than exact. The influence of the cylinder is propagated upstream on the flat plate a distance of 2 diameters and the ratio h/h_o increases to 8 at the stagnation line of the cylinder. The region of high heat transfer is washed downstream on each side of the cool region of the wake. The low heat transfer in the region of low-density separated flow in the wake is confined to a distance of less than 1 diameter; then h/h_o increases to almost 2.

Increasing the Reynolds number per foot by a factor of $2\frac{1}{2}$ at a Mach number of 3.51 as shown in figure 4 has a negligible effect on the area influenced by the cylinder but decreases h/h_0 at the stagnation point (of the cylinder) from $8\frac{1}{2}$ to $6\frac{1}{2}$.

The Mach number was varied with a constant Reynolds number per foot. The most significant effect was shown to be an increase of h/h_0 at the stagnation line of the cylinder from 5 at a Mach number of 2.65 to 8 at 3.51 with no systematic effect in the wake.

The heat transfer on the cylinder is presented in figure 5 as the ratio of the measured heat-transfer coefficient to the calculated heat-transfer coefficient based on free-stream conditions for laminar flow on a cylinder of infinite length as presented in reference 2. This ratio will be referred to hereinafter as h/h_L. The ratio is shown for $M = 2.65$ and 3.51 at the stagnation line; at three vertical distances from the flat plate the variation of the ratio about the forward $90°$ of the cylinder is shown. The shock pattern caused by the interaction of the cylinder bow shock with the flat plate, as shown in figure 16 of reference 3, causes a high-density separated flow and a resultant thickening of the boundary layer that causes a region of high heat transfer whose proximity to the flat plate increases with increasing Mach number. The portion of the cylinder uninfluenced by the flat plate is in good agreement with theory. There is no measurable effect of Reynolds number on the distribution of h/h_L on the cylinder.

The effect of locating the instrumented cylinder at several positions in the wake of a second cylinder was investigated at a Mach number of 3.51 and approximately $R = 2.8 \times 10^6$ per foot. The contour plot in figure 6 illustrates the heat-transfer distribution resulting from placing the instrumented cylinder 3.2 diameters downstream of a dummy cylinder. The region of high heating upstream of the dummy cylinder should be of the same magnitude as that for the single cylinder; the comparatively low indicated value of h/h_0 of 5 is due to the lack of instrumentation about this cylinder. The resultant wake and very mixed flow cause a reduction in heat transfer upstream of the instrumented cylinder. The thermocouple in the flat plate at the stagnation point indicates a value of h/h_0 of less than 4 in comparison with a value of 8 for the single cylinder. Figure 7 illustrates that the separated flow reduces the heat-transfer coefficient on the second cylinder; the value of h/h_L varies from 0.3 to 0.8 along the stagnation line. The circumferential plots indicate flow reattachment resulting in a value of h/h_L 25 to 50 percent higher than that predicted at the $45°$ and $90°$ stations.

In figure 8, the result of positioning the instrumented cylinder 6.4 diameters downstream of the dummy cylinder is shown. The relatively large distance between the two cylinders permits the flow field to reestablish a heat-transfer distribution similar to that for the single cylinder. The thermocouple on the flat plate at the stagnation line of the cylinder indicates a value of h/h_o of 6 as compared with the value of 8 for the single-cylinder configuration. The heat-transfer distribution on the instrumented cylinder in figure 9 indicates that the large influence of the wake of the dummy cylinder on the stagnation line noted in the preceding configuration is considerably damped and the overall distribution is similar to that for the single cylinder. The reattached flat-plate boundary layer is thinner and the region of high heating is closer to the flat plate than with the single-cylinder configuration. The circumferential distribution of h/h_L on the portion of the cylinder uninfluenced by the flat plate indicates that the measured values are less than predicted, and the deviation increases with increasing ψ.

Figure 10 shows the h/h_o distribution resulting from placing the instrumented cylinder 3.2 diameters downstream of the dummy cylinder and offset so that a line connecting the centers of the cylinders forms an angle of $26\frac{1}{2}^o$ with the free stream. Superposing the contour plot for the single cylinder on the dummy cylinder indicates that the instrumented cylinder is just downstream of the region of high heat transfer associated with the bow shock of the leading cylinder, and the thermocouple reading at the stagnation line is only slightly higher than that of the preceding configuration. The distribution of h/h_L on the cylinder shown in figure 11 indicates that the leading cylinder bow shock produces a slight increase in heat transfer closer to the flat plate than that associated with the single cylinder with maximum heating occurring at the edge of the boundary layer. The portion of the cylinder not influenced by the flat plate is in good agreement with theory.

In figure 12, the instrumented cylinder is 3.2 diameters downstream of the dummy cylinder, a line connecting the centers of the cylinders from an angle of 45° with the free stream. The region of elevated heating from the leading cylinder bow shock impinges on the instrumented cylinder between 0 and 90° and results in extremely high values of h/h_o ranging from 9 to 12 adjacent to the cylinder. The cylinder heat transfer shown in figure 13 indicates that the region of maximum heating along the stagnation line occurs some distance from the flat plate with a maximum h/h_L of $2\frac{3}{4}$. The circumferential plots indicate a value of h/h_L of 2 for angles up to 45°.

Exploratory tests have also been conducted on roughness elements that are small compared with the boundary-layer thickness. Figure 14 illustrates the skin of a sandwich-construction element that had been deformed by abnormal heating rates. A model was constructed to duplicate this surface with the bottom of the dimples 0.020 inch below the surface. Tests were conducted in the ceramic-heated jet (pilot model) with a free-stream Mach number of 4 and stagnation temperatures of approximately 2,500° F. The test specimen was the surface of a 30° wedge and resulted in a surface Mach number of 3 and a free-stream Reynolds number of 6×10^6 per foot. Detailed temperature measurements failed to indicate any significant change in the level of the heating in the region of the dimpled surface as compared with that of a smooth surface.

Similar tests were conducted on stainless-steel Phillips-type screwheads in a stainless-steel surface. The location of the screws in relation to the model surface is shown in the upper sketch in figure 15. In order to simulate normal manufacturing tolerances, the surfaces of the screws were 0.015 inch above the model surface, flush, and 0.015 inch below the surface. Thermocouples on the back face of the screwheads and temperature measurements of the surface made by a photographic technique showed that all the screwheads reached temperatures which averaged approximately 100° hotter than those of the adjacent skin. The photograph of the model in figure 16 was taken during the latter portion of the test; the luminescence is a function of temperature. With the assumption that the high screw temperatures resulted from the fact that the mass of the screw is substantially less than that for a cylinder of skin of equal face area, the screwhead temperature time history was computed, with consideration of the conduction across the metal-to-metal interface as outlined in reference 4 and the assumption that the heat transfer was the same as that of the adjacent skin. The results in figure 17 show good agreement with theory. In order to check the assumption that the screwhead temperature is dependent upon the area exposed to aerodynamic heating and the conduction across the interface, a second model, illustrated in the lower portion of figure 15, was constructed. All three plugs have the same volume, one plug was cylindrical, the other two plugs were tapered with a ratio of two to one. On face areas with the same test conditions as those used on the honeycomb deformed skin, the plug with the large area outboard had a temperature 100° greater and the inverted plug had a temperature of 100° cooler than the cylindrical plug that had the same temperature as the model skin.

CONCLUDING REMARKS

In conclusion, the presence of large protuberances that are only partially immersed in a turbulent boundary layer effects a large increase in heat transfer upstream and on each side of the protuberance wake.

Extreme care must be taken in locating a protuberance in the influence of another one. The ratio at a particular thermocouple of the heat-transfer coefficient for the flat plate with the protuberance to the heat-transfer coefficient of the flat plate alone can be as great as 12 in the more adverse location.

Langley Aeronautical Laboratory,
     National Advisory Committee for Aeronautics,
          Langley Field, Va., March 19, 1958.

REFERENCES

1. Tucker, Maurice: Approximate Calculation of Turbulent Boundary-Layer Development in Compressible Flow. NACA TN 2337, 1951.

2. Goodwin, Glen, Creager, Marcus O., and Winkler, Ernest L.: Investigation of Local Heat-Transfer and Pressure Drag Characteristics of a Yawed Cylinder at Supersonic Speeds. NACA RM A55H31, 1956.

3. Bloom, Martin H., and Pallone, Adrian: Heat Transfer to Surfaces in the Neighborhood of Protuberances in Hypersonic Flow. 1957 Heat Transfer and Fluid Mechanics Institute (Held at C.I.T.), Stanford Univ. Press, June 1957, pp. 249-278.

4. Barzelay, Martin E., Tong, Kin Nee, and Holloway, George F.: Thermal Conductance of Contacts in Aircraft Joints. NACA TN 3167, 1954.

FLAT-PLATE HEAT-TRANSFER MODEL
AND PROTUBERANCE
LANGLEY UNITARY PLAN WIND TUNNEL
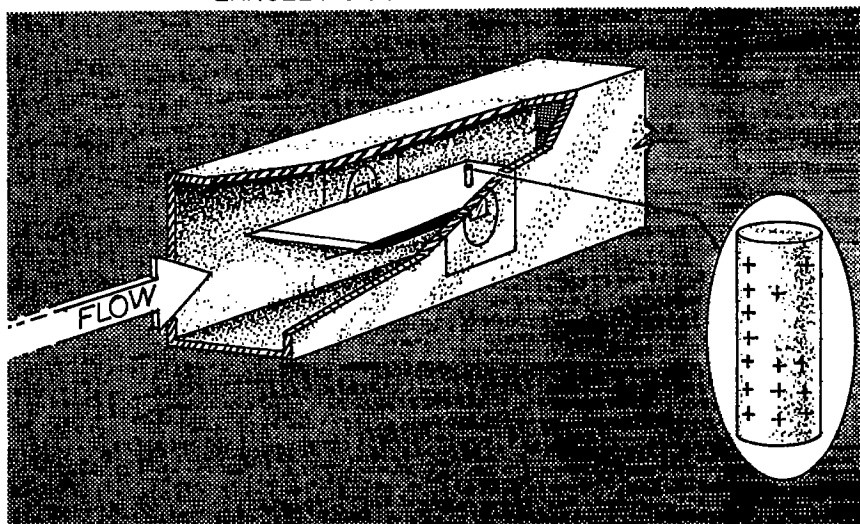
Figure 1

DISTRIBUTION OF STANTON NUMBER ALONG MODEL CENTER LINE
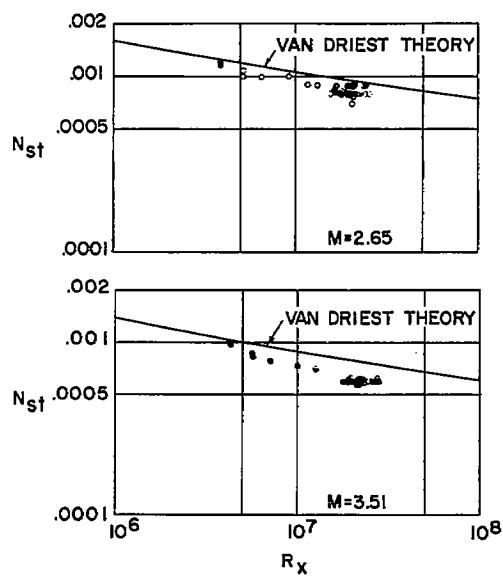
Figure 2

FLAT-PLATE HEAT TRANSFER

SINGLE CYLINDER; M = 3.51; R_x = 23.4 X 10^6
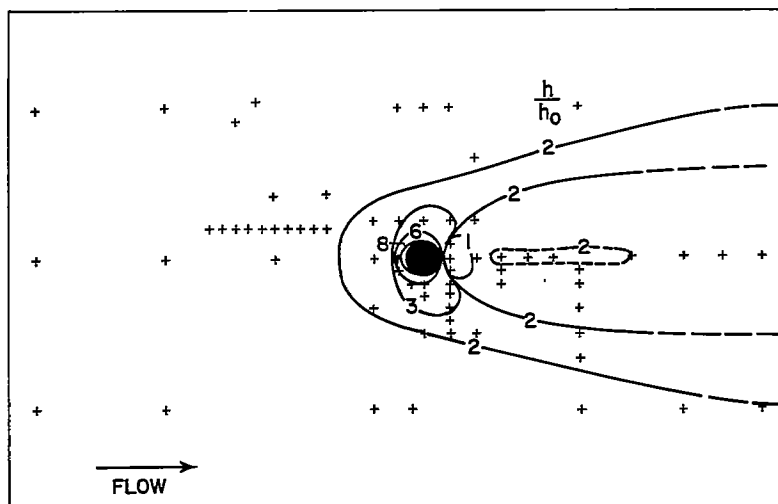
Figure 3

EFFECT OF REYNOLDS NUMBERS ON FLAT—PLATE HEAT TRANSFER

M = 3.51

Figure 4
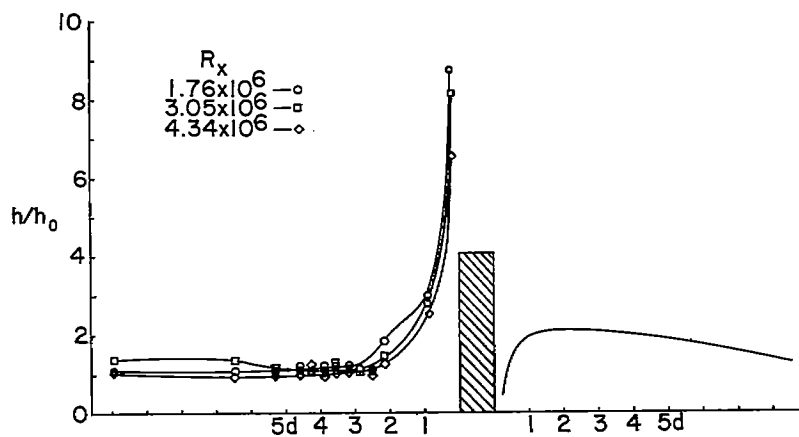
CYLINDER HEAT TRANSFER
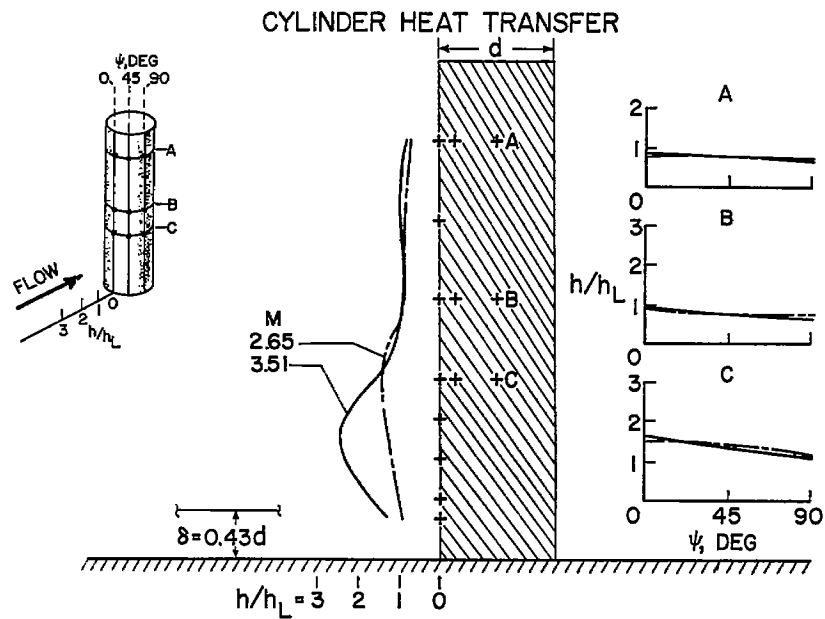
Figure 5

FLAT-PLATE HEAT TRANSFER
TANDEM CYLINDERS 3.2 d APART; M=3.51; R_x=21.6×10⁶

Figure 6

CYLINDER HEAT TRANSFER

Figure 7

FLAT-PLATE HEAT TRANSFER
TANDEM CYLINDERS SPACED 6.4d APART; M=3.51; $R_X = 21.6 \times 10^6$

Figure 8
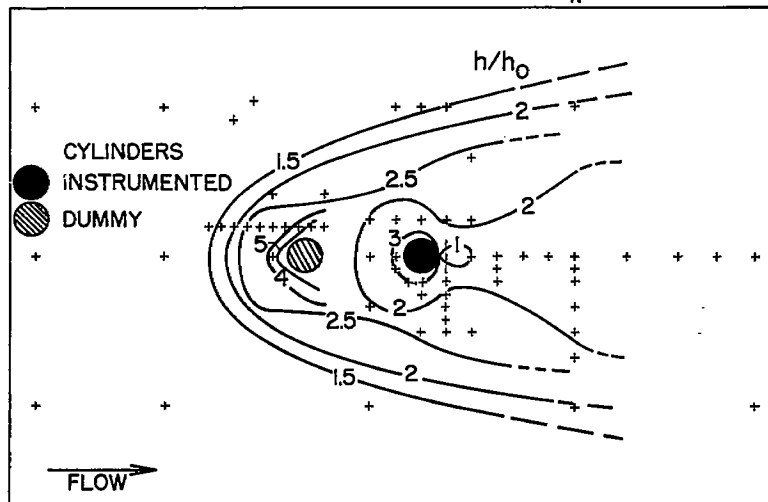
Figure 9
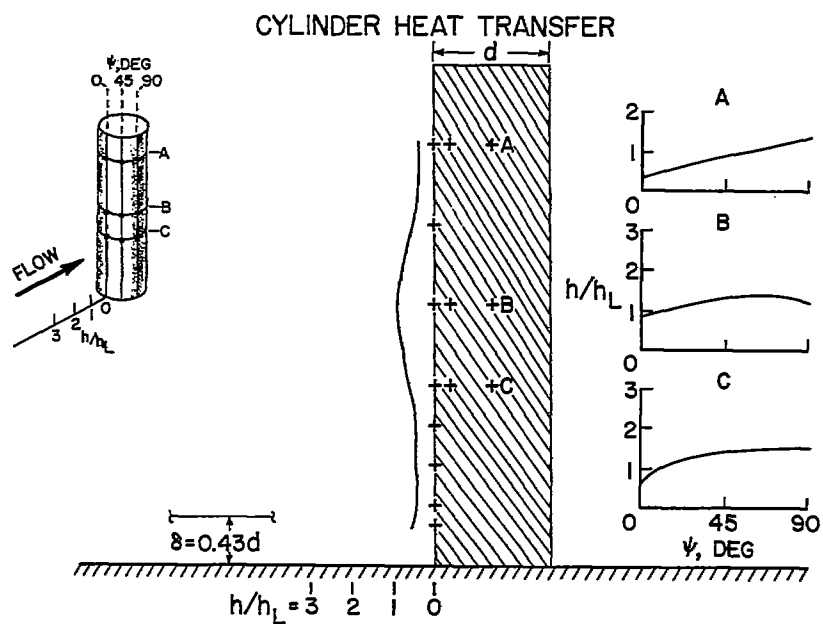
Figure 10
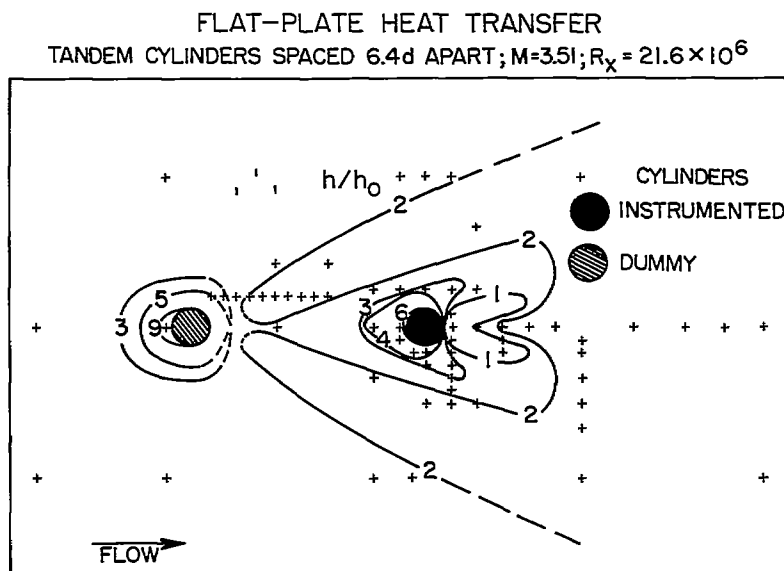
CYLINDER HEAT TRANSFER
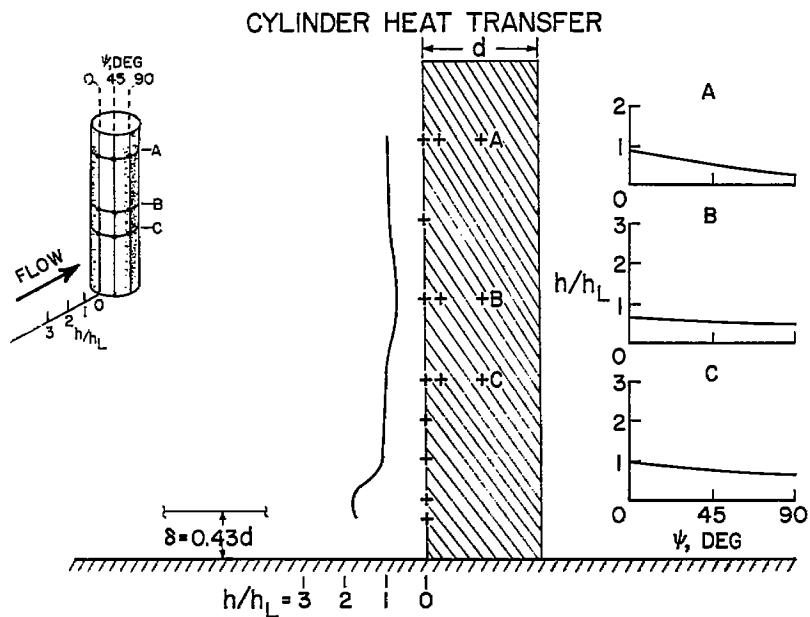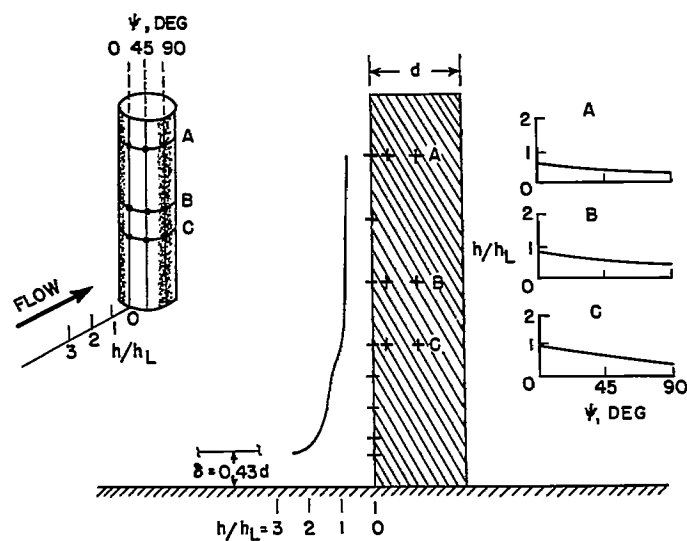
Figure 11

FLAT-PLATE HEAT TRANSFER

CYLINDERS WITH 45° OFFSET; $M = 3.51$; $R_X = 22.1 \times 10^6$

Figure 12

CYLINDER HEAT TRANSFER
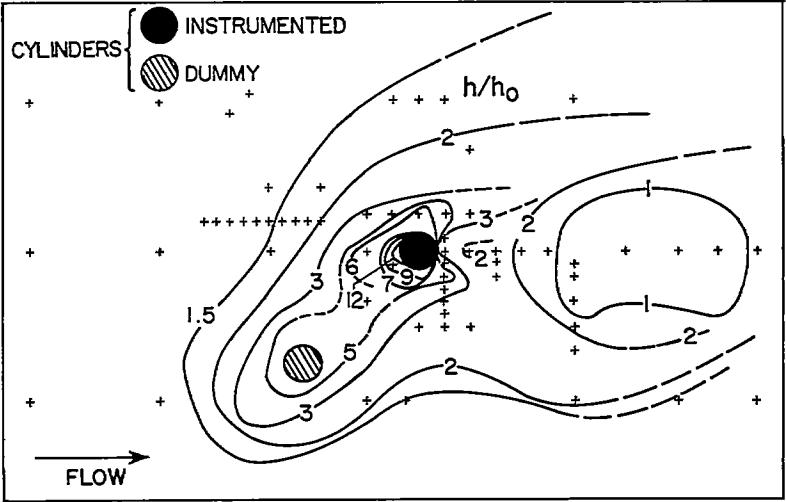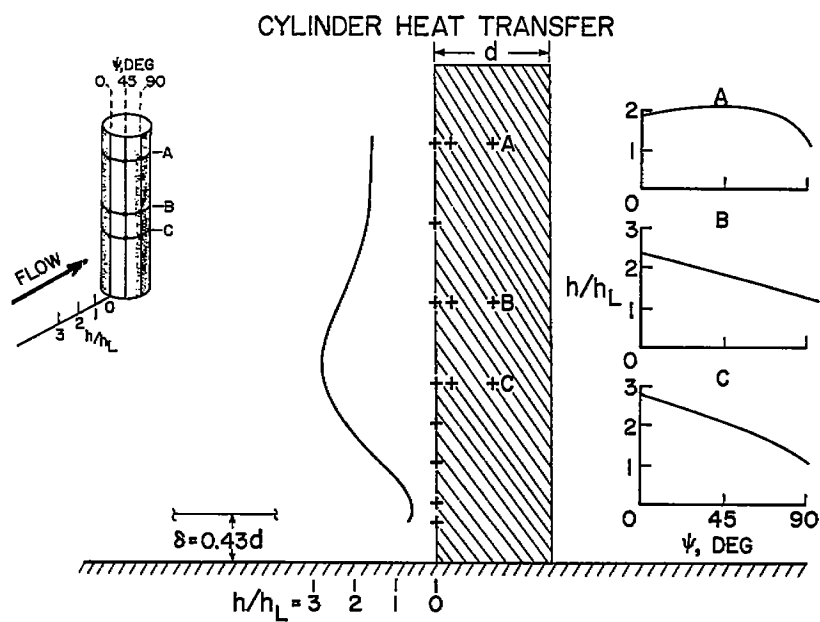
Figure 13

HONEYCOMB STRUCTURE AFTER HEATING
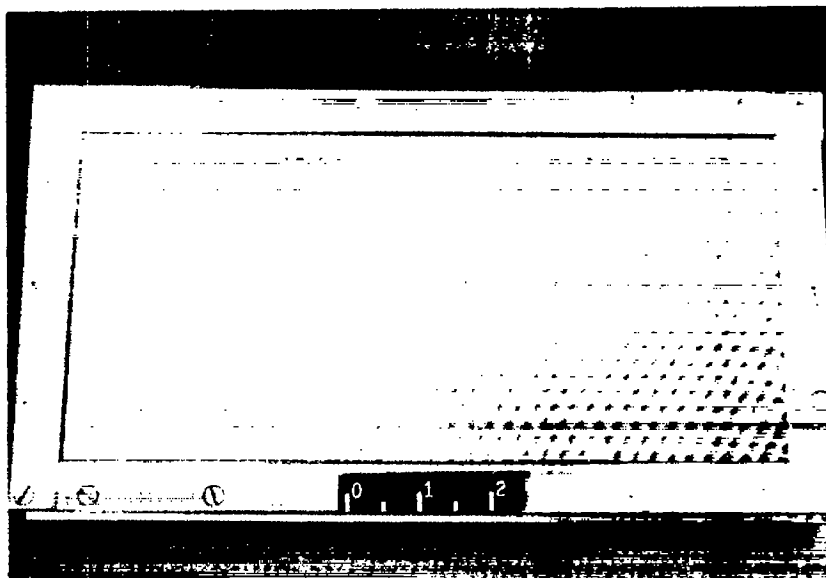
L-57-2192

Figure 14

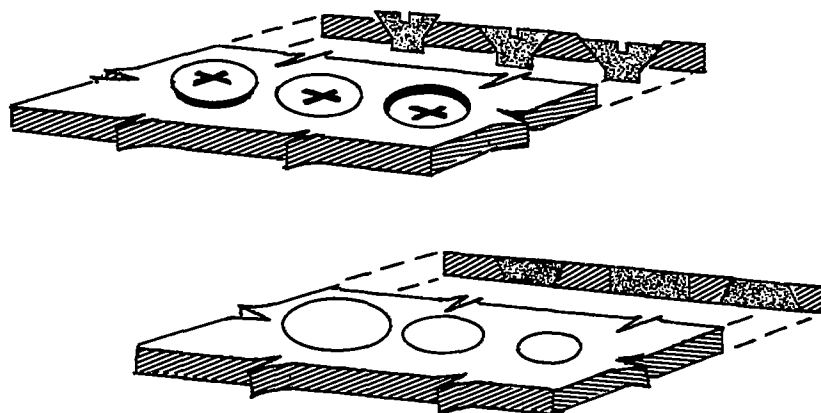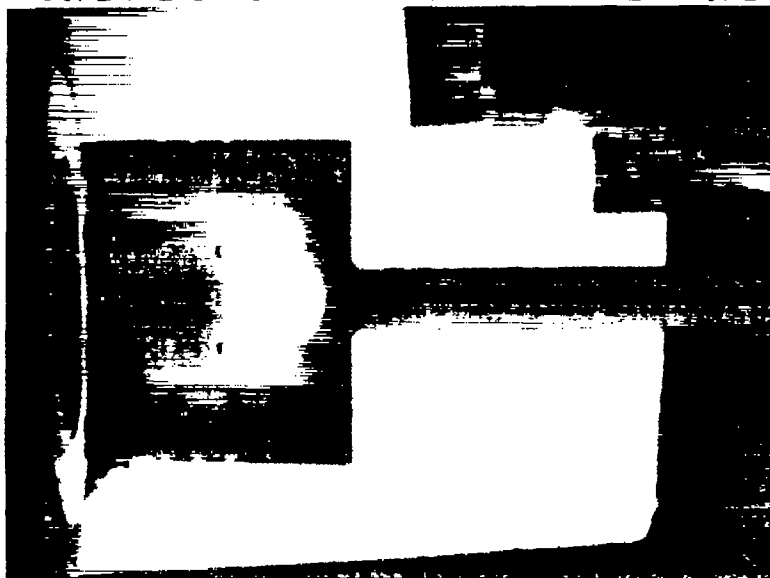SPECIMENS TESTED IN PILOT-MODEL
CERAMIC-HEATED AIR JET

M=4

Figure 15

SCREWHEAD MODEL AT ELEVATED TEMPERATURE
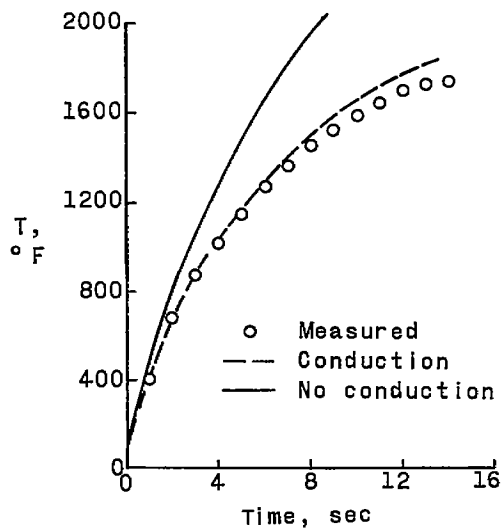

L-58-1656

Figure 16

COMPARISON OF CALCULATED AND MEASURED
TEMPERATURE TIME HISTORY OF SCREWHEADS

Figure 17